Field Quality in Fermilab-built Models of Quadrupole Magnets for the LHC Interaction Region

N. Andreev, T. Arkan, P. Bauer, R. Bossert, J. Brandt, S. Caspi, D.R. Chichili, J. Carson, J. DiMarco, S. Feher, A. Ghosh, H. Glass, V. V. Kashikhin, J. Kerby, M.J. Lamm, A. D. McInturff, A. A. Makarov, A. Nobrega, I. Novitski, T. Ogitsu, D. Orris, J.P. Ozelis, T. Peterson, R. Rabehl, W. Robotham, G. Sabbi, R. Scanlan, P. Schlabach, C. Sylvester, J. Strait, M. Tartaglia, J.C. Tompkins, G. Velev, S. Yadav, A.V. Zlobin

Abstract— **Superconducting quadrupole magnets for the interaction regions of the Large Hadron Collider are being developed by the US-LHC Accelerator Project. These 70 mm bore quadrupole magnets are intended to operate in superfluid helium at 1.9 K with a nominal field gradient of 215 T/m. A series of 2 m model magnets has been built and cold tested at Fermilab to optimize their design and construction and to study the performance of the magnets. Field measurements of the 8 model magnets and comparisons with the required field quality are reported in this paper.**

Index Terms—**magnetic fields, quadrupole, superconductivity**

I. Introduction

TO achieve a luminosity of 10^{34} $cm^{-2}s^{-1}$ at the LHC, special quadrupole magnets are required for the final focusing triplets in the interaction region [1]. These magnets must provide a field gradient of 215 T/m over a 70 mm bore with good field quality due to large and rapidly varying values of the β-function in the interaction region. Half of these inner triplet quadrupoles (MQXB) will be built and tested at Fermilab. The other half will be built at KEK. The design for the MQXB has been developed by a Fermilab-LBNL collaboration, and a short model magnet program completed to validate this design and construction techniques. Nine 2 m models have been built (HGQ01-09), of which eight were tested in superfluid helium at the Fermilab Vertical Magnet Test Facility. During testing, an extensive program of field harmonics measurements was executed. In this paper we present results of the measurements and compare them with calculations based on as-built magnet geometry.

II. MAGNET DESIGN

Figure 1 shows the magnet cross-section. The design is based on four two-layer coils connected in series, surrounded by collar and yoke laminations. No significant modifications to the design cross-section for these magnets were made during the magnet model program; however, the end regions underwent several design iterations [2]. The first five models were built with a four-block end configuration. A new five-block configuration which improves the mechanical stability of inner layer conductors during winding was implemented in models beginning with HGQ06. The new design also significantly improves field quality in the end region and reduces the peak field in the coil end.

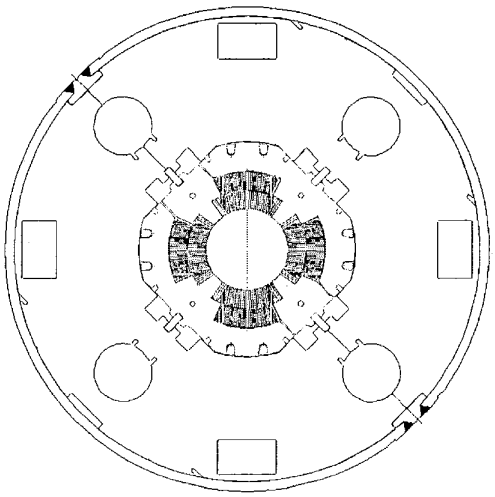

Fig. 1. Magnet cross-section. The coil bore diameter is 70 mm and the skin outside diameter 416 mm.

The initial model magnet collar and yoke design allowed for tuning shims to correct field errors. Shims were located in 8 rectangular cavities between the collars and yoke. In magnets HGQ01-05, these cavities were filled with a nominal shim package of half magnetic and half non-magnetic material. A scheme for tuning magnets was developed and tested with good success [3]. However, shims complicate construction and testing [2] of magnets. The field quality of HGQ05 was adequate "as-built", and a decision was made to eliminate tuning shims from the design pending testing of the remaining model magnets. Shims were not installed in HGQ05-08. The missing iron of the shims reduced the gradient by 1.1%, but produced no noticeable change in harmonics. HGQ09 was built with yoke laminations incorporating the iron of the nominal shim, returning the gradient to the design value. The regions occupied by the non-magnetic portion of the shim were

Manuscript received September 18, 2000. Work supported by the U.S. Department of Energy.

All authors are with Fermilab, P.O. Box 500, Batavia, IL 60510, USA, (email: schlabach@fnal.gov, (630 840-5037) except these.

S. Caspi, A. D. McInturff, G. Sabbi, R. Scanlan are with Lawrence Berkeley National Laboratory, Berkeley, CA, USA.

A. Ghosh is with Brookhaven National Laboratory, Upton, NY, USA.

T. Ogitsu is with KEK, Tsukuba, Japan.

J.P. Ozelis is with Jefferson Lab, Newport News, VA, USA.

TABLE I
Reference collision harmonics for MQXB (V2.0)

n	$<b_n>$	$d(b_n)$	$\sigma(b_n)$	$<a_n>$	$d(a_n)$	$\sigma(a_n)$
Straight section (L_{mag} 4.76 m)						
3	.0	.3	.8	.0	.3	.8
4	.0	.2	.8	.0	.2	.8
5	.0	.2	.3	.0	.2	.3
6	.0	.6	.6	.0	.05	.1
7	.0	.05	.06	.0	.04	.06
8	.0	.03	.05	.0	.03	.04
9	.0	.02	.03	.0	.02	.02
10	.0	.02	.03	.0	.02	.03
Lead end (L_{mag} 0.41 m)						
2	-	-	-	40.	-	-
6	2.	2.	.8	.0	.5	.2
10	-.2	.2	.1	.0	.1	.1
Return end (L_{mag} 0.33 m)						
6	.0	1.2	1.	-	-	-
10	-.25	.25	.1	-	-	-

left open to provide additional cooling. In addition, the 4 large circular cooling holes near the outer radius of the cross-section were reduced in size from 60 to 50 mm. This change in hole size does not effect iron saturation of the yoke so the field is unchanged. Since the field quality in magnets HGQ05-09 was good, a final decision was made to build production magnets with laminations identical to those used in HGQ09.

III. MEASUREMENT SYSTEM

Magnetic measurements presented in this paper were performed using a vertical drive, rotating coil system. Probes used have a tangential winding for measurement of higher order harmonics as well as dedicated dipole and quadrupole windings measuring the lowest order components of the field. These windings also allow for bucking the large dipole and quadrupole components in the main coil signal. Most measurements presented in this paper were made with a coil of 40.6 mm nominal diameter and a length of 82 cm. During testing of later magnets, a short probe with 25 mm nominal diameter and 4.3 cm length was used for longitudinal scans of the magnet, particularly in the end regions.

Coil winding voltages are read using HP3458 DVMs. An additional DVM is used to monitor magnet current. DVMs are triggered simultaneously by an angular encoder on the probe shaft, synchronizing measurements of field and current. Feed down of the quadrupole signal to the dipole is used to center the probe in the magnet.

IV. FIELD QUALITY ANALYSIS

In the straight section of the magnet, the field is represented in terms of harmonic coefficients defined by the power series expansion

$$B_y + iB_x = B_2 10^{-4} \sum_{n=1}^{\infty} (b_n + ia_n) \left(\frac{x+iy}{r_0} \right)^{n-1} \qquad (1)$$

TABLE II
Comparison of measured straight section harmonics (6 kA) with calculations based on as-built parameters.

n	HGQ			
	01	02	03	05
b_6, calc.	-4.24	-2.86	-1.39	-0.08
b_6, meas.	-3.91	-1.54	-1.02	-0.30
b_{10}, calc.	-0.14	-0.09	-0.04	0.01
b_{10}, meas.	-0.10	-0.10	-0.04	0.01
a_4, calc.	1.27	0.94	0.00	0.00
a_4, meas.	2.00	0.53	0.32	0.19
a_8, calc.	0.02	0.00	0.00	0.00
a_8, meas.	0.02	0.02	0.03	0.00

where B_x and B_y are the transverse field components, B_2 is the quadrupole field strength, b_n and a_n are the $2n$-pole coefficients (b_2=10^4) at the LHC reference radius r_o of 17 mm.[1] The coordinate system for magnetic measurement is defined in [2].

Table I shows the reference harmonics at collision for MQXB magnets developed at the beginning of the model magnet program. For each harmonic component, values of the mean, uncertainty in mean and standard deviation are listed. The table served the US-LHC collaboration and CERN as a reference for the discussion of field quality issues related to machine performance and interaction region systems layout during magnet development. Results of beam tracking studies evaluating the impact of magnet field errors on LHC dynamic aperture indicate that the values listed in Table I are acceptable from the machine performance standpoint [4].

As has been reported [5][6], large values for both allowed and unallowed harmonics were measured in early model magnets due to the thick coil shims required to obtain desired pre-stress, affecting b_6 and b_{10}, and coil size differences in the different quadrants, producing a_4 and a_8. Improvements in fabrication procedures [7] led to coils of more uniform size and modulus with corresponding improvement in field quality. Table II shows a comparison between measured harmonics and calculations based on as-built parameters for the harmonic components b_6, b_{10}, a_4 and a_8. Calculations and measurements are generally in good agreement.[2] In magnet HGQ05, all four harmonics are within the uncertainties specified by the reference table. Measured values of the harmonics are similarly small in HGQ06-09.

Table III shows the measured straight section harmonics up to the 20-pole for all models. In magnets HGQ05-9, all central harmonics are within one standard deviation of the random error specified in Table I. From the values in Table III, averages and standard deviations over the last 5 models have been obtained for each component (Table IV). All average values and standard deviations are

[1]Field harmonics in all tables are given in these units of 10^{-4} normalized to the main field.

[2]The measurements are made at a current of 6 kA where all non-geometric components (conductor magnetization, iron saturation, conductor displacement under Lorentz forces) are small. Moreover, the measurements at 6 kA do not differ significantly from those taken at higher currents.

TABLE III
Measured harmonics in the magnet straight section (6 kA).

	HGQ							
n	01	02	03	05	06	07	08	09
b_3	0.36	-0.70	1.04	0.72	0.25	0.18	0.61	0.71
b_4	0.26	0.18	0.14	0.00	0.09	0.01	-0.12	-0.05
b_5	-0.29	0.09	-0.34	-0.04	-0.11	-0.04	-0.01	0.08
b_6	-3.91	-1.54	-1.02	-0.30	-0.05	-0.45	-0.06	-0.28
b_7	-0.08	-0.01	-0.06	0.01	-0.03	0.02	-0.01	0.06
b_8	0.06	0.01	0.00	0.00	0.00	0.00	0.00	-0.01
b_9	0.04	0.00	0.00	0.00	0.00	-0.01	0.00	0.00
b_{10}	-0.10	-0.10	-0.04	0.01	0.00	-0.02	-0.01	-0.01
a_3	0.27	0.55	-0.30	0.12	-0.27	0.41	-0.01	0.35
a_4	2.00	0.53	0.32	0.19	-0.31	-0.50	-0.43	0.31
a_5	0.02	-0.17	0.26	0.05	-0.07	-0.24	0.12	-0.14
a_6	-0.08	0.03	0.07	-0.03	-0.05	-0.10	-0.03	0.04
a_7	-0.05	0.00	-0.03	0.01	0.00	0.07	0.00	0.02
a_8	0.02	0.02	0.03	0.00	0.00	0.01	-0.01	0.01
a_9	0.01	-0.01	0.01	0.00	0.00	0.01	-0.01	0.00
a_{10}	0.02	0.00	-0.01	0.00	0.00	0.00	0.00	0.00

within the limits specified in Table I.

The difference between harmonics measured during up and down ramp was small in magnets HGQ01-5, indicating small magnetization and eddy current effects [8]. However, in magnets HGQ06 and HGQ07, large differences between harmonics measured during up and down ramps were observed. These differences increased with increasing ramp rate [2]. For example, b_6 differed from up to down ramp by -1 unit when ramped at 10 A/s and -7 units when ramped at 80 A/s. Significant differences were present in all low order harmonics. Such ramp rate dependent field effects were also seen in HGQ08 and are due to eddy currents in the magnet coils. These eddy current field effects are consistent with measurements of energy losses during AC cycling of magnet power and significantly lower quench current at high ramp rate (Table V) [9]. The eddy currents are due to low strand crossover resistances in the coils of the 3 magnets.[3] Magnets HGQ06-08 were the first in the series using coils cured at simultaneous high temperature and pressure (Table V) resulting in the low crossover resistances [10]. Coils for HGQ09 were cured with a modified curing cycle (high temperature/low pressure followed by low temperature/high pressure). This change in the cure cycle produced coils with small eddy currents similar to those of HGQ01-5.

[3]Predictions for crossover resistance based on measured harmonics show low resistance and large coil to coil variations, explaining the non-allowed ramp dependent multipole components.

TABLE IV
Average and standard deviation of harmonics for HGQ05-09

n	$<b_n>$	$\sigma(b_n)$	$<a_n>$	$\sigma(a_n)$
3	0.49	0.26	0.12	0.28
4	-0.02	0.08	-0.15	0.37
5	-0.02	0.07	-0.06	0.15
6	-0.23	0.17	-0.03	0.05
7	0.01	0.03	0.02	0.03
8	0.00	0.00	0.00	0.01
9	0.00	0.00	0.00	0.01
10	-0.01	0.01	0.00	0.00

TABLE V
Quench current and b_6 as a function of coil curing cycle

	coil curing cycle		I_c	$\Delta b_6, 6kA$
	temperature	pressure	300 A/s	40 A/s
HGQ01	135°	low	10965	0.02
HGQ02	190°	low	11335	0.21
HGQ03	195°	low	11298	0.16
HGQ05	130°	low	10519	0.12
HGQ06	190°	high	6433	-1.04
HGQ07	190°	high	4487	-0.55
HGQ08	190°	high	3941	-0.72
HGQ09	190/135°	low/high	12946	0.13

End field calculations and measurements of HGQ01-06 were reported in [2]. Magnet HGQ06 had a new 5-block end design, reducing b_6 in the lead end by 35%. HGQ07-09 had the same 5-block design. A comparison of measured and calculated harmonics in the magnet ends is given in Table VI. As in the magnet straight section, the multipole components in the end regions are expressed in units of 10^{-4} of the quadrupole field.[4] The reference integration interval in z for harmonic coefficients in the magnet ends is defined to be [-0.57, 0.25] m for the return end and [1.31, 2.13] m for the lead end, matching the length of the measurement probe [11]. Measurements in the lead end of the 4 models with the new end design are quite consistent and agree well with calculations. Calculations of the field harmonics in the return end and corresponding measurements of HGQ09 with the 4.3 cm probe are also given. In both lead and return end the measured b_6 is 0.4 to 0.5 units lower than the predicted value. This discrepancy is believed to be due to local shims in the magnet end region not included in the calculation.

Injection takes place at fields (B_2) ranging from 12.3 to 14.1 T/m due to the different β^* in the different interaction regions. At these low levels of excitation (670 to 770 A), persistent currents result in an additional component of the allowed harmonics. Averaged over the magnet series, the additional b_6 at 770 A (670 A) is -1.2 (-1.6) units

[4]The magnetic length L_m of the end region is defined as the length of straight section which would provide an equivalent integrated gradient and defines the appropriate weighting factor for end and body harmonics in the integral field of the magnet.

TABLE VI
Calculated and measured harmonics of the magnet end regions.

	HGQ					
	lead end					ret.
harmonic	05	06	07	08	09	09
b_6, calc.	5.4	3.5				0.1
b_6, meas.	8.0	3.1	3.1	3.1	3.0	-0.6
b_{10}, calc.	-0.4	-0.1				-0.1
b_{10}, meas.	-0.2	-0.1	-0.1	-0.0	-0.1	-0.1
a_6, calc.	-0.1	-0.7				-
a_6, meas.	-0.3	-0.4	-0.3	-0.4	-0.4	0.3
a_{10}, calc.	0.0	0.0				-
a_{10}, meas.	0.0	0.0	0.0	0.0	0.0	0

TABLE VII
Reference harmonics for MQXB (V3.2)

n	$<b_n>$	$d(b_n)$	$\sigma(b_n)$	$<a_n>$	$d(a_n)$	$\sigma(a_n)$
Straight section - collision (L_{mag} 4.76 m)						
3	0	0.60	0.27	0	0.23	0.27
4	0	0.15	0.27	0	0.20	0.27
5	0	0.15	0.10	0	0.15	0.10
6	0	0.45	0.20	0	0.07	0.03
7	0	0.04	0.02	0	0.03	0.02
8	0	0.01	0.02	0	0.01	0.01
9	0	0.01	0.01	0	0.01	0.01
10	0	0.01	0.01	0	0.01	0.01
Straight section - injection						
3	0	0.60	0.27	0	0.23	0.27
4	0	0.15	0.27	0	0.20	0.27
5	0	0.15	0.10	0	0.15	0.10
6	-1.6 (670 A)	0.60	0.60	0	0.07	0.03
	-1.2 (770 A)	0.60	0.50	0	0.07	0.03
7	0	0.04	0.02	0	0.03	0.02
8	0	0.01	0.02	0	0.01	0.01
9	0	0.01	0.01	0	0.01	0.01
10	0	0.01	0.01	0	0.01	0.01
Lead end - inj. & collision (L_{mag} 0.41 m)						
3	0	0.90	0.80	0	0.90	0.80
4	0	0.70	0.80	0	0.70	0.80
5	0	0.40	0.50	0	0.40	0.50
6	3.10	0.20	0.07	-0.35	0.20	0.07
7	0	0.10	0.04	0	0.10	0.04
8	0	0.03	0.03	0	0.03	0.03
9	0	0.01	0.01	0	0.01	0.01
10	-0.05	0.01	0.01	0	0.01	0.01
Return end - inj. & collision (L_{mag} 0.33 m)						
3	0	0.90	0.80	0	0.90	0.80
4	0	0.70	0.80	0	0.70	0.80
5	0	0.40	0.50	0	0.40	0.50
6	-0.4	0.30	0.07	0	0.20	0.07
7	0	0.10	0.04	0	0.10	0.04
8	0	0.03	0.03	0	0.03	0.03
9	0	0.01	0.01	0	0.01	0.01
10	-0.05	0.05	0.01	0	0.01	0.01

with an RMS of 0.5 (0.6). Decay of the field at constant current have been observed. For example, b_6 decays by 0.4 units during a 30 minute 800 A plateau with 90% of that occurring during the first 15 minutes. Note that, while we report these effects, they have negligible impact on machine performance as the number of insertion quadrupoles is a small fraction of all magnets.

V. REFERENCE HARMONICS TABLE

At the beginning of the short model program, a reference harmonics table (Table I) was established based on the analysis of magnet field errors due to mechanical tolerances, magnetization effects, and magnetic measurement accuracy. Consideration was also given to results from previous magnet series production and a safety margin included to account for uncertainties in the development of the new design. Improvements in coil fabrication and a new end design have produced magnets with field errors systematically smaller than those originally anticipated (Table IV). A revised field quality table based on measured data from the model magnets has been developed (Table VII). Body harmonics are based on measurements of HGQ05-09. Lead end harmonics are based on measurements of HGQ06-09, all of which use the 5-block end design. Since return end harmonics have been measured in only one magnet, the same uncertainties and randoms as for the lead end are used. The end b_6 systematic is based on measurements and includes a 0.4 units difference with respect to the design value. Based on the new reference table, the number of local correction elements has been reduced as was the required strength of others.

VI. CONCLUSIONS

Improvement in coil production techniques led to steady improvement in field quality in the first few magnets. Field harmonics in the last 5 magnets of the magnet series have been consistently small. Evaluation of field measurements made during the series has led to a new reference table for field quality which is primarily based on data and is expected to characterize MQXB production. Tracking studies using this reference table have led to elimination of some corrector elements local to the interaction region and to a reduction in the strength of others. Comparison of calculation to measurements shows good agreement in integral body and end region harmonics. Eddy current effects leading to large ramp rate dependent multipole components in HGQ06-08 were eliminated in HGQ09 through use of a modified coil curing cycle giving high crossover resistance between cable strands. Measurements of HGQ07-09 confirm the improved end field quality of the new 5-block design introduced in HGQ06.

REFERENCES

[1] "LHC Conceptual Design", CERN AC/95-05 (LHC).

[2] N. Andreev, et. al., "Field Quality in Fermilab-built Models of High Gradient Quadrupole Magnets for the LHC Interaction Regions", IEEE Trans. Appl. Supercond., Vol. 10, No. 1, March, 2000.

[3] G. Sabbi, et. al., "Correction of High Gradient Quadrupole Harmonics with Magnetic Shims", IEEE Trans. Appl. Supercond., Vol. 10, No. 1, March, 2000.

[4] J. Wei, et al., "Interaction Region Local Correction for the Large Hadron Collider", 1999 Particle Accelerator Conference, New York, April 1999.

[5] R. Bossert, et. al., "Analyis of Magnetic Measurements of Short Model Quadrupoles for the LHC Low-β Insertions", EPAC'98, Stockholm, June 1998.

[6] R. Bossert, et. al., "Magnetic Measurements of the Fermilab High Gradient Quadrupoles for the LHC Interaction Regions", IEEE Trans. Appl. Supercond., Vol. 9, No. 7, June, 1999.

[7] N. Andreev, et. al., "Study of Kapton Insulated Superconducting Coils Manufactured for the LHC Inner Triplet Model Magnets at Fermilab", IEEE Trans. Appl. Supercond., Vol. 10, No. 1, March, 2000.

[8] N. Andreev, et. al., "Field Quality of Quadrupole R&D Models for the LHC IR", 1999 Particle Accelerator Conference, New York, April 1999.

[9] S. Feher, et. al., "Quench and Mechanical Performance of Fermilab Quadrupole Models for the LHC Inner Triplets", this conference.

[10] J. Kerby, et. al., "Status of the LHC Inner Triplet Quadrupole Program at Fermilab", this conference.

[11] G. Sabbi, et. al., "Magnetic Field Analysis of the First Short Models of a High Gradient Quadrupole for the LHC Interaction Regions", Proc. MT-15 Conf., Beijing, 1997.